

A variable temperature Fe³⁺ electron paramagnetic resonance study of Sn_{1-x}Fe_xO₂ (0.00 ≤ x ≤ 0.05)

S. K. Misra^{a)} and S. I. Andronenko

Physics Department, Concordia University, 1455 de Maisonneuve Boulevard West, Montreal QC H3G 1M8, Canada

K. M. Reddy, J. Hays, A. Thurber, and A. Punnoose^{b)}

Department of Physics, Boise State University, Boise, Idaho 83725-1570

(Presented on 11 January 2007; received 31 October 2006; accepted 22 November 2006; published online 10 May 2007)

X-band (~9.5 GHz) electron paramagnetic resonance (EPR) studies of Fe³⁺ ions in Sn_{1-x}Fe_xO₂ powders with 0.00 ≤ x ≤ 0.05 at various temperatures (5–300 K) are reported. These samples are interesting to investigate as Fe doping (≤5%) produces ferromagnetism in SnO₂ [A. Punnoose *et al.*, Phys. Rev. B **72**, 054402 (2005)], making it a promising ferromagnetic semiconductor at room temperature. The EPR spectrum at 5 K can be simulated reasonably well as the overlap of spectra due to seven magnetically inequivalent Fe³⁺ ions: four low-spin (*S*=1/2) and three high-spin (*S*=5/2) ions, characterized by different spin-Hamiltonian parameters, overlapped by three broad ferromagnetic resonance spectra. The three high-spin ions, situated substitutionally in the interior of nanodomains, are characterized by smaller zero-field splitting (ZFS) parameters *D* and *E*, so that all their energy levels are populated at 5 K. On the other hand, the four low-spin ions are situated interstitially at the surfaces of nanodomains. They are characterized by much larger ZFS, so that only their lowest Kramers doublets are occupied at 5 K. Based on this simulation, it is concluded that the observed spectra at different temperatures can be reproduced by changing appropriately the relative overlaps of the various paramagnetic and ferromagnetic characters, which remain present over the temperature range studied. © 2007 American Institute of Physics.

[DOI: 10.1063/1.2709752]

I. INTRODUCTION

Tin dioxide (SnO₂) is an attractive system for a wide variety of practical applications,^{1–6} being a chemically stable transparent oxide semiconductor with a band gap of ~3.6 eV. It has been shown that Fe doping produces ferromagnetism in SnO₂,⁷ thus making it a promising ferromagnetic semiconductor at room temperature. This material, therefore, has the potential for use in spintronic devices such as spin transistors, spin light-emitting diodes (LEDs), very high-density nonvolatile semiconductor memory, and optical emitters with polarized output,^{8–11} in which both the spin and charge of the particles play important roles. It is believed that oxygen vacancies and substitutional incorporation are important to produce ferromagnetism in semiconductor oxides¹² doped with transition metal ions. The synthesis details of the samples investigated here have been described elsewhere.⁷ The present paper reports detailed electron paramagnetic resonance (EPR) investigations of these samples aimed to understand how Fe ions are incorporated into the SnO₂ lattice and their interaction with environment. Based on quantitative magnetic measurements reported earlier,⁷ it was shown that chemically synthesized Sn_{1-x}Fe_xO₂ powders exhibit room-temperature ferromagnetism for x ≤ 0.05 when prepared in the 350–600 °C range. A high Curie temperature

T_C of 850 K was observed for these samples.⁷ In this work, only samples prepared at 600 °C are investigated.

II. RESULTS AND DISCUSSION

Figure 1 shows the EPR spectra at 5 K as recorded on a Bruker X-band spectrometer, equipped with an Oxford Instruments variable temperature accessory for the samples doped with different concentrations of Fe (0.4%, 0.7%, 2.6%, and 4.7%). For the samples with 0.7% and 4.7% Fe, measurements were also carried out as a function of temperature in the 5–350 K range. Figure 2 shows the representative set of these spectra for the 0.7% and 4.7% Fe doped samples.

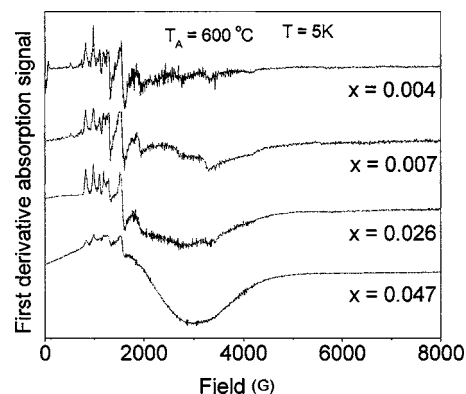


FIG. 1. First derivative EMR signals recorded at 5 K for different Fe dopings in SnO₂ (Sn_{1-x}Fe_xO₂) prepared at 600 °C.

^{a)} Author to whom correspondence should be addressed; electronic mail: skmisra@alcor.concordia.ca

^{b)} Electronic mail: apunnoos@boisestate.edu

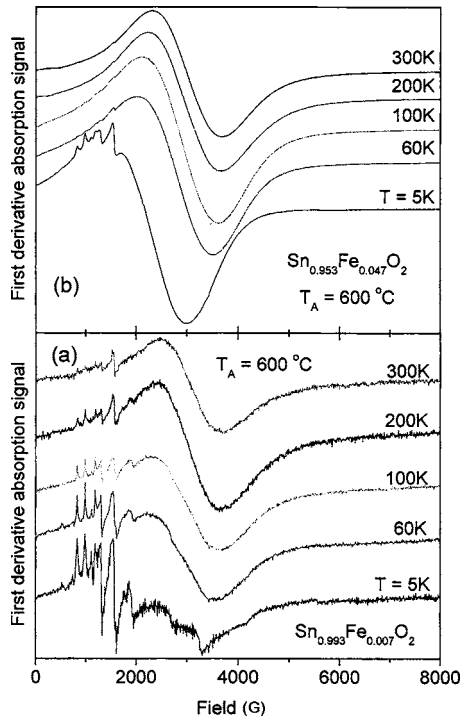


FIG. 2. First derivative EMR absorption signals recorded at different temperatures for (a) 0.7% and (b) 0.47% Fe-doped SnO_2 sample prepared at $T_A=600^\circ\text{C}$.

A visual inspection of the various spectra and fitting trials reveal that there exists an overlap of three types of spectra: (i) three broad ferromagnetic resonance (FMR) lines due to ferromagnetically coupled Fe^{3+} ions; (ii) four interstitially incorporated low-spin Fe^{3+} ions on the surface of nanodomains with effective spin $S=\frac{1}{2}$ characterized by large zero-field splittings (ZFS), so that only the lowest Kramers doublet ($M=\pm 1/2$) is significantly populated at all temperatures of observation; and (iii) three substitutionally incorporated high-spin Fe^{3+} ions are presumably situated in the interior of nanodomains with effective spin $S=5/2$, characterized by small ZFS so that all the three Kramers doublets ($M=\pm 5/2, \pm 3/2, \pm 1/2$) are populated. The reasons for these assignments, based on previous EPR studies,^{13,14} are as follows. At substitutional sites in single crystals of SnO_2 , only the high-spin state of Fe^{3+} was ob-

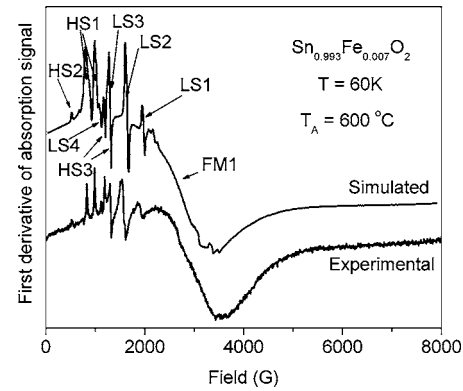


FIG. 3. Simulated and experimentally recorded first derivative FMR absorption spectra for 0.7% Fe doped SnO_2 prepared at 600°C and measured at 60 K. Here LS=low spin line, HS=high-spin line, and FM1=FMR line.

served. Thus these ions are situated in the interior of nanodomains. The g -tensor values for the interstitial site observed here correspond to those reported in Ref. 14. On the other hand, the low-spin states observed here are due to Fe^{3+} ions situated interstitially on the surface of nanodomains, which are not observed in single crystals.

The spin-Hamiltonian characterizing the spin-1/2 state is $H_S = \mu_B \mathbf{B} \cdot \mathbf{g} \cdot \mathbf{S}$, which represents the Zeeman interaction, with \mathbf{B} , \mathbf{g} , and μ_B being the magnetic-field intensity, g tensor, and the Bohr magneton, respectively. On the other hand, the spin-Hamiltonian characterizing the spin-5/2 state is $H_S = g\mu_B \mathbf{B} \cdot \mathbf{S} + D[S_z^2 - (1/3)S(S+1)] + E[S_x^2 - S_y^2]$, where D and E are axial and nonaxial ZFS parameters, respectively. The spectra were simulated, as shown in Fig. 3 along with that observed experimentally at 60 K for the 0.7% Fe doped sample prepared at 600°C , using WIN-EPR software (Bruker) assuming the three types of contributions described above. The values of the spin-Hamiltonian parameters used, linewidths, spin assignments, and relative intensity employed to simulate the observed EPR spectrum are listed in Table I. Figure 4 shows the shape of the spectra expected for a FM resonance, and EPR spectra for low-spin ($S=1/2$), and high-spin ($S=3/2$) Fe^{3+} ions. The spectrum intensity was calculated using the overlap $(\text{FM1}+\text{FM2}+\text{FM3})+(\text{LS1}+\text{LS2}+\text{LS3}+\text{LS4}+\text{HS1}+\text{HS2}+\text{HS3}) \times \exp(-0.014B)$, where the exponential factor is related to the Boltzmann population dis-

TABLE I. Spin-Hamiltonian parameters, width, spin assignment, site, and relative intensity employed to simulate the observed EMR spectrum. (* indicates $g_z < 1.0$ so it is outside the range of the field employed in this work.)

EMR line	g_x	g_y	g_z	D (Gauss)	E (Gauss)	Intensity	Width (Gauss)	Assignment	Host sites
LS1	3.4	3.4	*			1.35	15	Low spin Fe^{3+}	Interstitial
HS1	2.0	2.0	2.0	645	-185	0.43	40	High spin Fe^{3+}	Substitutional
HS2	2.0	2.0	2.0	700	-190	0.05	8	High spin Fe^{3+}	Substitutional
LS2	4.1	4.1	*			2.19	15	Low spin Fe^{3+}	Interstitial
LS3	5.2	5.2	*			1.00	15	Low spin Fe^{3+}	Interstitial
HS3	2.0	2.0	2.0	610	-165	0.5	15	High spin Fe^{3+}	Substitutional
LS4	5.7	5.7	*			0.48	15	Low spin Fe^{3+}	Interstitial
FM1	3.3	3.3	3.3			0.1	2000	FMR	Nanoparticles
FM2	1.6	1.6	1.6			0.04	7000	FMR	Nanoparticles
FM3	2.35	2.35	2.35			0.06	1000	FMR	Nanoparticles

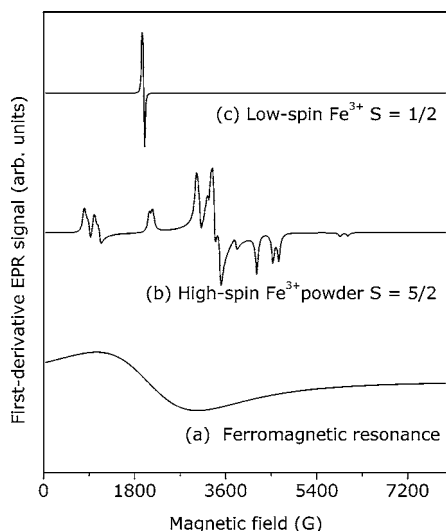


FIG. 4. Simulated spectra for (a) simulated first derivative broad resonances (FMR), (b) that due to a low-spin ($S=1/2$) Fe^{3+} ion at an interstitial site, and (c) that due to a high-spin ($S=5/2$) Fe^{3+} ion at a substitutional site.

tribution of energy levels. Based on this simulation, it is concluded that the observed spectra at different temperatures can be reproduced by changing appropriately the relative overlaps of the various paramagnetic and ferromagnetic characters, which remain present over the temperature range studied.

In SnO_2 , each tin ion is octahedrally surrounded by six oxygen ions at equal distances. When a $3d$ impurity ion, such as Fe^{3+} , substitutes for the Sn^{4+} ion, it might cause an axial distortion due to the difference in the size and charge of the ions. Fe^{3+} ions in SnO_2 preferably substitute for Sn^{4+} ions in octahedral sites. Dusausoy *et al.*¹³ reported four Fe sites in single crystals of Fe doped SnO_2 due to different charge compensation mechanisms. Three of these four centers were due to substitutional Fe^{3+} ions. The fourth Fe^{3+} center is coupled to a Nb^{5+} ion present as an impurity. In our EMR studies, we also observed three similar substitutional Fe^{3+} sites. In addition, we observed four interstitial low-spin locations on the surfaces of nanodomains. This is not too surprising considering the significantly higher Fe concentrations employed in our samples and the nanoscale particle size. In the nanoscale size range, the role of the particle surface enhances significantly and additional features different from the bulk form are well expected.

The nature and spectral parameters of the FMR signals are similar to those reported for magnetic nanoparticle systems below their blocking temperatures.^{15–17} The shift of the observed signal to lower fields and changes in the linewidth are related to the anisotropy in nonspherical particles with a statistical distribution of sizes and shapes.^{15–17} Transmission electron microscopy⁷ showed the presence of nonspherical nanoscale particles in these samples. Using magnetometry measurements, clear evidence for room-temperature ferro-

magnetism was observed in samples with $\leq 5\%$ Fe, and the systematic increase in the intensity of the FMR component in these samples supports these results.⁷

III. CONCLUSIONS

The simulations presented here help bring an understanding to the main EPR spectral features. The EPR measurements presented in this paper reveal that Fe doping results in both a ferromagnetically ordered component as well as isolated paramagnetic Fe^{3+} ions incorporated into the SnO_2 lattice. Evidence for both substitutional and interstitial incorporation of Fe was observed in the EPR spectra. The presence of both paramagnetic spins and ferromagnetically ordered components has been reported to be present in transition metal doped semiconductor oxide systems.^{7,12} A detailed microscopic analysis of the observed spectra will require an exorbitant effort, which is not warranted over and above the main features of the magnetic properties already deduced.

ACKNOWLEDGMENTS

At Boise State University, this research was supported by the NSF-CAREER award (DMR-0449639), NSF-Idaho-EPSCoR Program, and the National Science Foundation under Award Nos. EPS-0447689 and DMR-0321051, and one of the authors (S.K.M.) is grateful to the Natural Sciences and Engineering Research Council of Canada for partial financial support.

- ¹E. J. H. Lee, C. Ribeiro, T. R. Giraldo, E. Longo, E. R. Leite, and J. A. Varela, *Appl. Phys. Lett.* **84**, 1745 (2004).
- ²N. Chiodini, A. Paleari, D. DiMartino, and G. Spinolo, *Appl. Phys. Lett.* **81**, 1702 (2002).
- ³P. G. Harrison, N. C. Lloyd, and W. Daniell, *J. Phys. Chem. B* **102**, 10672 (1998).
- ⁴S.-C. Lee, J.-H. Lee, T.-S. Oh, and Y.-H. Kim, *Sol. Energy Mater. Sol. Cells* **75**, 481 (2003).
- ⁵S. A. Pianaro, P. R. Bueno, E. Longo, and J. A. Varela, *J. Mater. Sci. Lett.* **14**, 692 (1995).
- ⁶E. A. Bondar, S. A. Gormin, I. V. Petrochenko, and L. P. Shadrina, *Opt. Spectrosc.* **89**, 892 (2000).
- ⁷A. Punnoose, J. Hays, A. Thurber, M. H. Engelhard, R. K. Kukkadapu, C. Wang, V. Shuthanandan, and S. Thevuthasan, *Phys. Rev. B* **72**, 054402 (2005).
- ⁸G. A. Prinz, *Science* **282**, 1660 (1998); *J. Magn. Magn. Mater.* **200**, 57 (1999).
- ⁹S. A. Chambers and R. F. C. Farrow, *MRS Bull.* **28**, 729 (2003).
- ¹⁰S. J. Pearton *et al.*, *J. Appl. Phys.* **93**, 1 (2003).
- ¹¹N. Lebedeva and P. Kuivalainen, *J. Appl. Phys.* **93**, 9845 (2003).
- ¹²J. M. D. Coey, A. P. Douvalis, C. B. Fitzgerald, and M. Venkatesan, *Appl. Phys. Lett.* **84**, 1332 (2004).
- ¹³Y. Dusausoy, R. Ruck, and J. M. Gaite, *Phys. Chem. Miner.* **15**, 300 (1988).
- ¹⁴W. Rhein and C. Rosinski, *Phys. Status Solidi B* **118**, 667 (1972).
- ¹⁵K. Nagata and A. Ishihara, *J. Magn. Magn. Mater.* **104–107**, 1571 (1992).
- ¹⁶A. Punnoose, M. S. Seehra, J. van Tol, and L. C. Brunel, *J. Magn. Magn. Mater.* **288**, 168 (2005).
- ¹⁷A. Punnoose and M. S. Seehra, in *EPR in the 21st Century*, edited by A. Kawamori, J. Yamauchi, and H. Ohta (Elsevier Science, New York, 2002), p. 162.